Crosstalk, Noise, and Stability Analysis of DWDM Channels Generated by Injection Locking Techniques

B. Cai, L. A. Johansson, C. F. C. Silva, S. Bennett, and Alwyn J. Seeds, *Fellow, IEEE*

***Abstract*—In this paper, theory and experimental results for wavelength-division-multiplexing (WDM) channel generation, formed by multi-line optical injection locking, is presented. A small-signal model to deal with wide-spectral-band optical injection problems has been developed. Based on this model, the crosstalk noise of an injection-locked laser in a coherent WDM system is assessed analytically. Experimental results on locking range, stability, and crosstalk noise confirms the modeling results, which indicate that stable and low-noise channels can be generated by this approach.**

***Index Terms*—Optical injection locking, optical transmitters, wavelength-division multiplexing (WDM).**

I. Introduction

MOST current commercial dense wavelength-division multiplex (DWDM) systems operate with 2.5- or 10-Gb/s channel capacity. Due to a number of optical fiber and optical device impairments, the narrowest channel spacing used is currently 50 GHz. These figures lead to commercial spectral efficiencies limited to 0.2 b/s/Hz.

One option to increase spectral efficiency is to increase the individual channel capacity to 40 Gb/s. The technology involves utilization of high-complexity components, with technological and physical impairments regarding group velocity and polarization mode dispersion in fiber, leading to limitations on the achievable transmission distance [1].

Another option is to reduce channel spacing. Apart from nonlinear interactions between the modulated optical carriers and the fiber-optic transmission medium, limitations here arise also from DWDM components. When reducing channel spacing to 25 GHz or less in a 10-Gb/s system, strict tolerances for center wavelength drift of components and lasers over operating temperature, aging, and measurement uncertainties apply. First, the passive control of several hundred fixed wavelength lasers within such a tight margin easily becomes impractical. Second, the technical difficulty of fast and accurate wavelength allocation for wavelength agile components also increases with the reduced channel spacing.

One approach that can overcome the above difficulties is the use of a coherent channel forming scheme [2]. In a densely spaced wavelength-multiplexing transmission system, channels can be formed by injection locking a group of lasers to an optical comb, as shown in Fig. 1. Two absolute frequency references drive the optical frequency comb generator to produce an output spectrum with exactly spaced comb lines and absolutely stable central wavelength [3]. The former is set by a synthesized microwave reference, with frequency stability <1 Hz. The latter is set by a reference laser stabilized by atomic or molecular absorption techniques, which can achieve stability <0.2 kHz. The generated optical comb spectrum is then utilized as a stable frequency reference for fixed wavelength or tunable optical sources, forming optical channels by optical injection locking. The principle has been demonstrated using four input spectral lines from a laser, intensity modulated at 1 GHz [4].

Injection-locking techniques have been used for spectral control and frequency stabilization of semiconductor lasers since 1980 [5], [6] and provide promising results in various areas [7]–[10]. Much theoretical work has been performed to reveal the properties of injection-locked semiconductor lasers [11]–[14]. The case of a slave laser under injection from several laser sources is analyzed in [15]. In most of the work, it is assumed that injected light is concentrated in a narrow spectral line and, therefore, can be considered as quasi-monochromatic light, that is, a monochromatic signal with small amplitude or phase noise. The noise is assumed to be sufficiently small that small-signal approximation will be valid. However, in this application, such an assumption is no longer valid. In this case, the optical injection power is distributed in a group of evenly spaced spectral lines, which represent different channels, and the slave laser is locked onto a selected channel. The nonselected channels will to some degree influence the output of the slave laser. In a real system, this influence will be described as crosstalk noise between channels. With a channel spacing as small as 10 GHz, such noise may not necessarily be negligible. On the other hand, however, the spacing between channels is far too large for the noise to be estimated with a conventional single-frequency small-signal approach.

The locking stability is another important issue to be addressed, as it has a direct impact on the reliability and design of a DWDM system. In this case, although the influence of adjacent channels that are far beyond the slave laser locking

Manuscript received April 15, 2003; revised July 31, 2003. This work was supported in part by the U.K. EPSRC PHOTON project.

B. Cai was with the Department of Electronic and Electrical Engineering, University College London, WC1E 7JE London, U.K. He is now with JDS Uniphase.

L. A. Johansson was with the Department of Electronic and Electrical Engineering, University College London, WC1E 7JE London, U.K. He is now with the Department of Electrical and Computer Engineering, University of California, Santa Barbara, CA 93106 USA (e-mail: leif@ece.ucsb.edu).

C. F. C. Silva was with the Department of Electronic and Electrical Engineering, University College London, WC1E 7JE London, U.K. He is now with McKinsey.

S. Bennett was with the Department of Electronic and Electrical Engineering, University College London, WC1E 7JE London, U.K. He is now with DiCon Fiberoptics, Inc., Richmond, CA 94804 USA.

A. J. Seeds is with the Department of Electronic and Electrical Engineering, University College London, WC1E 7JE London, U.K. (e-mail: a.seeds@ee.ucl.ac.uk).

Digital Object Identifier 10.1109/JLT.2003.819787

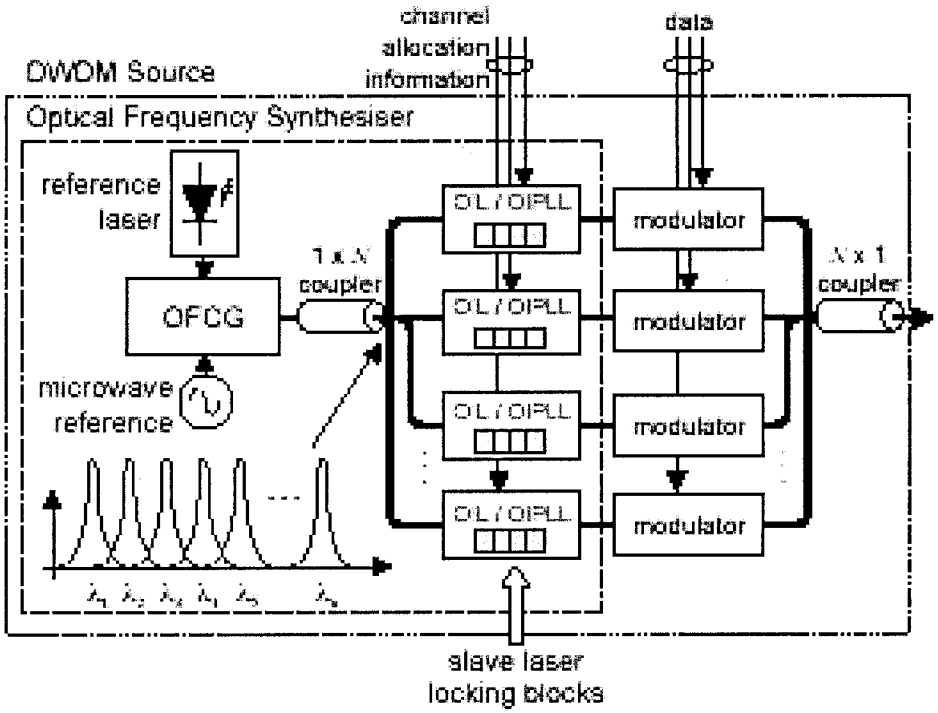

Fig. 1. Proposed scheme.

range can be ignored, the characteristics of distributed feedback (DFB) lasers have to be taken into account.

In this paper, the single-frequency small-signal model has been extended to cover the multichannel strong injection case and estimate the crosstalk noise. When a laser is locked on a selected channel, not only the relatively small noise in that channel but also the adjacent channels, which have considerable injection power but are separated by far more than the locking range from the selected channel, can be treated with the small-signal approach.

This paper is structured as follows. In Section II and III, numerical and analytical models for noise and stability for Fabry–Pérot (FP) lasers are presented as the foundation of further analysis. Based on this foundation, analytical modeling of DFB lasers using the effective parameter approach is performed in Section IV. Experiments to validate the theory and their results are also presented and compared with the theoretical model in Section IV.

II. FP Lasers With Wide Spectral Optical Injection

A. General Rate Equations and Large Signal Solutions

Due to the presence of much stronger injection optical power, the slave laser spontaneous emission can be ignored. If we express the electric field with a reference frequency ω_0 and complex amplitude E as $E(t)\exp(j\omega_0 t)$, the laser cavity rate equations in electric field-carrier number format are [16]

$$\frac{dE}{dt} = \left[j\Delta\omega + \frac{1}{2}\left(G - \frac{1}{\tau_p}\right)\right]E + \frac{1}{\tau_0}E^{\text{in}} \tag{1}$$

$$\frac{dN}{dt} = M - \frac{N}{\tau_e} - GP \tag{2}$$

where E^{in} is the electric field of injected light at the slave laser facet centralized at a reference frequency ω_0, $G = \tau_p^{-1} + G_n(N - N_f) + G_p(P - P_f)$ is the gain per unit time, G_n is the differential gain, N and N_f are the carrier population and its free running value, $G_p = \partial G/\partial P$ is the parameter standing for spectral hole burning and lateral carrier diffusion, P and P_f are the total photon number in the cavity and its free running value, τ_p and τ_e are the photon and spontaneous carrier lifetimes, $\Delta\omega = \omega_f - \omega_0 + \alpha G_n(N - N_f)/2 + \beta G_p(P - P_f)/2$ is the effective frequency offset from the laser free-running longitudinal mode angular frequency ω_f, α is the laser linewidth enhancement factor, β reflects photon-induced refractive index change and is normally considered equal to α for FP lasers, τ_0 is the laser cavity round-trip time, and M is the carrier injection rate.

We can simplify (1) and (2) using the above relations to have

$$\frac{dE}{dt} = \left[j\Delta\omega_0 + \frac{1 + j\alpha}{2}\Delta G\right]E + \frac{E^{\text{in}}}{\tau_0} \tag{3}$$

and

$$\frac{d\Delta N}{dt} + \frac{\Delta N}{\tau_e} + \frac{\mu_0 n_g}{h\nu c\tau_p}\left(|E|^2 - |E_0|^2\right) + \Delta G\frac{\mu_0 n_g |E|^2}{h\nu c} = 0 \tag{4}$$

and

$$\Delta G = G_n\Delta N + G_p\frac{\mu_0 n_g^2}{h\nu c}\left(|E|^2 - |E_0|^2\right) \tag{5}$$

where μ_0 is permeability in vacuum, ν is light emission frequency, c is light speed in a vacuum, and n_g is the group refractive index of laser waveguide. Equations (3) and (4) are a set of nonlinear differential equations and can be linked by (5) and solved numerically in the time domain using the Runge–Kutta–Fehlberg method for a variety of injection E^{in}.

B. Small-Signal Assumption and Linearization

Although the solution can be found by simply solving the above large signal nonlinear differential equation set numerically, a simple analytical solution is preferred to identify clearly the influence of each individual parameter and derive the models for more complicated lasers such as DFB lasers. Such a solution can be obtained by proper small-signal assumptions and linearization of (1) and (2).

When the injected optical power is not concentrated at a single frequency ω_0, the injection field can be written as $E^{\text{in}} = E_0^{\text{in}} + e^{\text{in}}(t)$, where E_0^{in} is a constant representing the noise-free injection field at frequency ω_0; $e^{\text{in}}(t)$ is a function of time representing the injection field at the other frequencies. Instead of requiring $e^{\text{in}}(t)$ itself to be small, we require that the perturbance induced by the perturbation field $e^{\text{in}}(t)$ in the slave laser be small. This requirement can be met if $e^{\text{in}}(t)$ satisfies either of the following: 1) its amplitude is much smaller than E_0^{in} or 2) it is far away from the the slave laser locking frequency range. Under both situations, the slave laser will be effectively locked with E_0^{in}, and the perturbance caused by $e^{\text{in}}(t)$ in the slave laser can be dealt with small-signal approximation. To apply such an approximation and linearize (1) and (2), let $E = E_0 + e(t)$, $\Delta\omega = \Delta\omega_0 + (\alpha/2)G_n n(t) + (\beta/2)G_p(|E|^2 - |E_0|^2)$, $N = N_0 + n(t)$, and $M = M_0 + m(t)$, where E_0, N_0, $\Delta\omega_0$, and M_0 are the steady-state solutions of E, N, $\Delta\omega$, and M when the slave laser is locked on E_0^{in} without the perturbation injection field $e^{\text{in}}(t)$; $e(t)$ and $n(t)$ are the slave laser field and carrier number deviation from their steady-state values E_0^{in} and N_0 caused by the perturbation injection $e^{\text{in}}(t)$. To keep the completeness of the analysis, we also introduce $m(t)$ as the carrier injection rate perturbance, similar to $e^{\text{in}}(t)$. The small perturbance requirement will be met if $m(t)$ satisfies either of the following: 1) it is much smaller than M_0 or 2) its frequency is much higher than the carrier dumping rate defined as $\Gamma_e = 1/\tau_e + G_n P_0$. The steady-state equations are obtained from (1) and (2) by assuming perturbance-free photon and carrier injections $E^{\text{in}} = E_0^{\text{in}}$, $M = M_0$ and using the steady-state conditions $dE/dt = 0$, $dN/dt = 0$

$$j\Delta\omega_0 + \frac{1}{2}\left(G_0 - \frac{1}{\tau_p}\right) = -\frac{E_0^{\text{in}}}{\tau_0 E_0} \tag{6}$$

$$\frac{N_0}{\tau_e} + G_0 P_0 = M_0 \tag{7}$$

where G_0 is the steady-state gain. Under the first-order approximation, the optical power change due to the perturbation injection $e^{\text{in}}(t)$ can be linked to the slave laser field by

$$P - P_0 = 2P_0 \text{Re}\left\{\frac{e(t)}{E_0}\right\}. \tag{8}$$

Using (6)–(8) and the above definitions, (1) and (2) can be linearized as

$$\frac{de}{dt} + \frac{E_0^{\text{in}}}{E_0\tau_0}e(t) - \frac{1+j\alpha}{2}G_n E_0 n(t) - \frac{1+j\beta}{2}G_p E_0 2P_0 \text{Re}\left\{\frac{e(t)}{E_0}\right\} = \frac{e^{\text{in}}(t)}{\tau_0} \tag{9}$$

$$\frac{dn}{dt} + \Gamma_e n(t) + 2P_0 \text{Re}\left\{\frac{e(t)}{E_0}\right\}(G_p P_0 + G_0) = m(t) \tag{10}$$

defining $\xi_n = ((1 + j\alpha)/2)G_n$ and $\xi_p = (1 + j\beta/2)G_p$ as the complex differential and nonlinear gain to reflect the influence of carrier and photon numbers on the real and image parts of the index, (9) and (10) can be rewritten as

$$\frac{de}{dt} + \frac{E_0^{\text{in}}}{E_0\tau_0}e(t) - E_0\xi_n n(t) - E_0\xi_p 2P_0 \text{Re}\left\{\frac{e(t)}{E_0}\right\} = \frac{e^{\text{in}}(t)}{\tau_0}$$

$$\frac{dn}{dt} + \Gamma_e n(t) + 2P_0 \text{Re}\left\{\frac{e(t)}{E_0}\right\}[G_0 + G_p P_0] = m(t).$$

To simplify the above equations further, we normalize the field with E_0 and time with τ_0

$$\frac{de}{dt} + E_0^{\text{in}}e(t) - \xi_n n(t) - \xi_p 2P_0 \text{Re}\{e(t)\} = e^{\text{in}}(t) \tag{11}$$

$$\frac{dn}{dt} + \Gamma_e n(t) + 2P_0 \text{Re}\{e(t)\}[G_0 + G_p P_0] = m(t) \tag{12}$$

or in matrix format

$$\left(\frac{d}{dt} + \overline{\mathbf{D}}\right)\begin{bmatrix} e(t) \\ e'(t) \\ n(t) \end{bmatrix} = \begin{bmatrix} e^{\text{in}}(t) \\ e^{\text{in}'}(t) \\ m(t) \end{bmatrix} \tag{13}$$

where

$$\overline{\mathbf{D}} = \begin{bmatrix} E_0^{\text{in}} - \xi_p P_0 & -\xi_p P_0 & -\xi_n \\ -\xi_p^* P_0 & E_0^{in^*} - \xi_p^* P_0 & -\xi_n^* \\ (G_0 + G_p P_0)P_0 & (G_0 + G_p P_0)P_0 & \Gamma_e \end{bmatrix}. \tag{14}$$

C. The Range and Stability of the Locking

With close examination of (6) and (7), we find that G_0, P_0, and N_0 only have real value solutions within a certain range. This can be interpreted as the range in which the injected light has significant influence on the N and P of the lasing mode. This range is normally defined as the locking range. Equation 13 is valid only when the injection E_0^{in} is within the locking range. When $\alpha = \beta$, the locking range is simply defined by

$$|\omega_f - \omega_0| \le \left|\frac{E_0^{\text{in}}\sqrt{\alpha^2 + 1}}{E_0\tau_0}\right| \tag{15}$$

and the expression will become much more complicated for $\alpha \neq \beta$.

Within the locking range, the locking may not necessarily be dynamically stable. As a linear system defined by (13), the dynamic stability of the slave laser can be assessed from its characteristic matrix $\overline{\mathbf{D}}$. For a dynamically stable system, the eigenvalues of $\overline{\mathbf{D}}$ must fall into the first and fourth quadrant of complex plane.

D. Small-Signal Solutions in Frequency Domain

Equation (13) as linear system equations can be solved in the frequency domain. Taking Fourier transform for both sides, we have

$$\begin{bmatrix} j\omega + E_0^{\text{in}} - \xi_p P_0 & -\xi_p P_0 & -\xi_n \\ -\xi_p^* P_0 & j\omega + E_0^{in^*} - \xi_p^* P_0 & -\xi_n^* \\ (G_0 + G_p P_0)P_0 & (G_0 + G_p P_0)P_0 & j\omega + \Gamma_e \end{bmatrix} \times \begin{bmatrix} e(\omega) \\ e^*(-\omega) \\ n(\omega) \end{bmatrix} = \begin{bmatrix} e^{\text{in}}(\omega) \\ e^{in^*}(-\omega) \\ m(\omega) \end{bmatrix}. \tag{16}$$

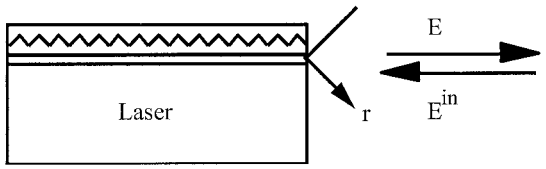

Fig. 2. DFB laser as a mirror with gain.

Notice here that Fourier transform properties for conjugate complex function pair are used. Equation (16) is a general solution for photon and carrier injection problems satisfying the small perturbance approximation. The solution of (16) is quite tedious but can be greatly simplified when the carrier injection perturbance $m(\omega) \equiv 0$ and the injection frequency detuning $\Delta\omega_0 \equiv 0$. In such a case (16) can be solved as

$$e(\omega) = \frac{e^{\text{in}}(\omega) + Z(\omega)\left[e^{\text{in}}(\omega) + e^{in^*}(-\omega)\right]}{j\omega + E_0^{\text{in}}} \tag{17}$$

where $Z(\omega) = Z_n(\omega)Z_p(\omega)$ and

$$Z_n(\omega) = -\frac{\xi_n P_0(G_0 + G_p P_0)}{(j\omega+\Gamma)^2 + \Omega^2}, \quad Z_p(\omega) = \frac{\xi_p P_0(j\omega+\Gamma_e)}{(j\omega+\Gamma)^2 + \Omega^2} \tag{18}$$

where $\Gamma = (E_0^{\text{in}} - G_p P_0 + \Gamma_e)/2$ and $\Omega = \sqrt{P_0^2 G_n^2[G_0 + G_p P_0]^2 - (\Gamma - \Gamma_e)^2}$ are the decay rate and angular frequency of relaxation oscillations.

III. DFB Lasers With Distributed Optical Injection

To deal with DFB and other lasers with complicated structures, we can use similar methods to those of Tromborg *et al.* [17]. At one facet of the laser, we treat the laser as a active mirror (shown in Fig. 2). Ignoring spontaneous emission, the emission field can be expressed in frequency domain as

$$E(\omega) = r(\omega)E^{\text{in}}(\omega) \tag{19}$$

where r_ω is the equivalent reflectivity coefficient. With the first-order approximation

$$\frac{\mathrm{r_0}}{\mathrm{r}} = 1 - \frac{\partial \ln(\mathrm{r})}{\partial\omega}\omega - \frac{\partial \ln(\mathrm{r})}{\partial \mathrm{N}}\mathrm{n} - \frac{\partial \ln(\mathrm{r})}{\partial \mathrm{P}}\mathrm{p} \tag{20}$$

where the static solution for noise-free injection E_0^{in} is $E_0(\omega_0) = r_0(\omega_0)E_0^{\text{in}}(\omega_0)$, we have

$$\left(1 - \frac{\partial \ln \mathrm{r}}{\partial\omega}\omega\right)\frac{\mathrm{e}(\omega)}{\mathrm{E_0}} - \frac{\partial \ln \mathrm{r}}{\partial \mathrm{N}}\mathrm{n}(\omega) - \frac{\partial \ln \mathrm{r}}{\partial \mathrm{P}}\mathrm{p}(\omega) = \frac{\mathrm{e^{in}}(\omega)}{\mathrm{E_0^{in}}}. \tag{21}$$

For carrier number, the possible nonuniform local distribution of carrier and photon, in general, has to been considered

$$\frac{dN}{dt} = M - \frac{N}{\tau_e} - \int_{\text{cavity}} G(\bar{r})\rho(\bar{r})d\bar{r} \tag{22}$$

where ρ is photon density. If the perturbance can be approximately assumed uniform through the cavity and we let

$$\tau_0 = j\frac{\partial \ln r}{r_0 \partial\omega} \tag{23}$$

$$\xi_n = \frac{\partial \ln r}{\tau_0 r_0 \partial N} \tag{24}$$

$$\xi_p = \frac{\partial \ln r}{\tau_0 r_0 \partial P} \tag{25}$$

$$P_0 = \frac{\mu_0}{h\nu c}\int_{\text{cavity}} |E(r)|^2 n_g^2(r)dr \tag{26}$$

$$G_0 = \langle G(r)\rangle_{\text{cavity}} \tag{27}$$

by normalizing time and field by τ_0 and E_0, respectively, and using the relation $\mathrm{p(t)} = \mathrm{P(t)} - \mathrm{P_0} \approx 2\mathrm{P_0Re\{e(t)/E_0\}}$, we have

$$\left(\mathrm{j}\omega + \mathrm{E_0^{in}}\right)\mathrm{e}(\omega) - \xi_\mathrm{n}\mathrm{n}(\omega) - \xi_\mathrm{p}\mathrm{P_0}[\mathrm{e}(\omega) + \mathrm{e}^*(-\omega)] = \mathrm{e^{in}}(\omega) \tag{28}$$

$$(\mathrm{j}\omega + \Gamma_\mathrm{e})\mathrm{n}(\omega) + (\mathrm{G_0} + \mathrm{G_p P_0})\mathrm{P_0}[\mathrm{e}(\omega) + \mathrm{e}^*(-\omega)] = \mathrm{m}(\omega). \tag{29}$$

It is noticed that (28) and (29) are identical with (11) and (12) for FP lasers. With equivalent parameters defined in (23)–(27), a DFB or other types of lasers with complicated longitudinal structures can be treated as FP lasers. It is also noticed that τ_0 has a small imaginary part that reflects effective gain change with emission optical frequency. Such an effect can be ignored with a laser operating near longitudinal mode ω_s, as we did in FP laser analysis.

The effective parameters τ_0, ξ_n, ξ_p, and the steady-state solution of the total photon population P_0 and gain G_0 in the laser resonator for different laser structures can be obtained with the transmission-line method. In the Appendix, we detail the calculation for a typical DFB laser structure.

IV. Modeling and Experimental Results

A. Locking Range and Stability

When the adjacent comb lines are far beyond the slave laser locking range, their influence can be ignored. Viewing the entire laser as a mirror with gain and wavelength selectivity, the effective reflection ratio, under the steady state, can be calculated using a transmission-line approach [17] and is a function of carrier density N and detuning frequency ω_0. For a given detuning frequency ω_0, the minimum injection required for locking is determined by the minimum value of $|E_0^{\text{in}}/E_0|^2 = |r_0^{-2}(\omega_0)|$. For a typical DFB laser (with second-order grating, length of 322 μm, effective index of 3.23, K factor of 23/cm, 0.2% and 30% reflection on its facets, respectively, estimated linewidth enhancement factor of 5.4, and internal loss of 50/cm), the locking range calculated in such a way is plotted in Fig. 3. The small-signal equations [(9)–(12) and (28) and (29)] only exist within such a range, given by the area falling outside the regions marked as "unlocked" in the figure.

Even within the locking range, due to the gain-index coupling effect quantified by the Henry factor α, the locking may not be dynamically stable. With a small-signal approximation derived

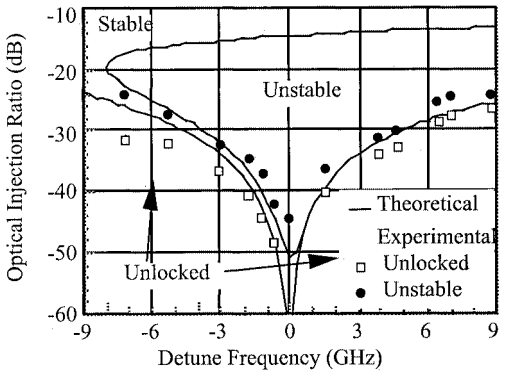

Fig. 3. DFB laser locking and stable range.

from the steady-state solutions, the dynamic locking stability is determined by evaluating the eigenvalues of small-signal differential equations. Away from very low or very high injection ratio, the region of dynamically stable locking is significantly reduced in comparison to the locking range calculated above, as shown by the region marked "stable" in Fig. 3. Fig. 3 shows good agreement between the calculated and measured results of the locking and stable range of a typical DFB laser, with parameters as above.

It is interesting to observe that with very weak or strong injection, the locking will be stable over the whole locking range. For very weak injection, the injection-induced gain change in the laser cavity is so small that the related index change becomes insignificant. For the strong injection, the injection ratio is such that the slave laser works almost like a semiconductor optical amplifier.

When the adjacent lines fall within the locking range, they will influence the locking stability. The steady-state solution/small-signal approach can then no longer be used. Fortunately, within a narrow spectral region, a DFB laser can be simplified to an equivalent FP laser. With such simplification, the related large signal rate equations can be solved numerically in the time domain using the Runge–Kutta–Fehlberg method. Fig. 4 shows that the locking becomes unstable when comb spacing f is reduced. Further results show that beyond the locking range, adjacent lines have very little influence on stability.

B. Channel Crosstalk

For comb spacing much greater than the locking range, the adjacent lines do not affect the locking stability but do pass through the slave laser and are present in the output causing channel crosstalk noise. First, we estimate the crosstalk interference from only one adjacent channel. Assume that the optical injection consists of two spectral lines, separated by frequency ω_i, representing two channels. The frequency of one of the spectral lines coincides with the locking center frequency, that is, $\Delta\omega_0 \equiv 0$. Then, the injection field can be expressed as $E^{in}(t) = E_0^{in} + a_i \exp(j\omega_i t)$. Taking $e^{in}(\omega) = a_i\delta(\omega - \omega_i)$ and $m(\omega) = 0$ (assuming no carrier injection perturbance) into (17), we find that the crosstalk noise is distributed at two frequencies: a main peak at frequency $\omega_0+\omega_i$ and a much weaker image peak

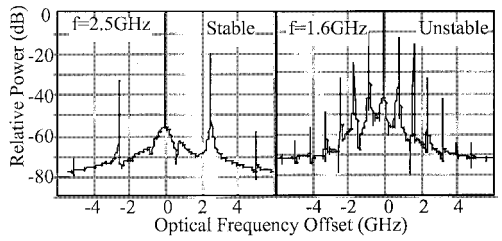

Fig. 4. FP laser large signal solutions.

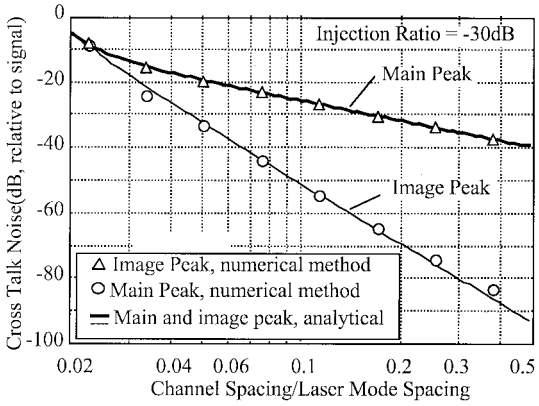

Fig. 5. FP laser comparison of numerical and analytical approaches.

at frequency $\omega_0 - \omega_i$. The amplitude of the main peak at $\omega_0+\omega_i$ is

$$e^{+} = \frac{a_i + Z(\omega_i)\frac{a_i}{2}}{j\omega_i + E_0^{in}}. \tag{30}$$

The amplitude of the image peak at $\omega_0 - \omega_i$ is

$$e^{-} = -\frac{Z(-\omega_i)\frac{a_i^*}{2}}{j\omega - E_0^{in}}. \tag{31}$$

To validate the small-signal assumption applied in the above equations, the large-signal nonlinear rate equations were solved numerically using Runge–Kutta–Fehlberg finite-element integration methods [18] using representative parameters for an injection-locked Hitachi HLP 1400 F-P type semiconductor laser, given by laser emission wavelength $\lambda = 0.83\ \mu$m, cavity length $L = 300\ \mu$m, group refractive index $n_g = 4.3$, round-trip time $\tau_0 = 2Ln_g/c$, internal distributed loss $\alpha_a = 45/$cm, facet reflectivity $R = 0.31$, photon lifetime calculated by $\tau_p = \tau_0/[\alpha_a L - \ln(R)]$, differential gain $G_n = 5750/$s, and spontaneous carrier lifetime $\tau_e = 2.2$ ns. Default values for other parameters are the linewidth enhancement factor $\alpha = 5.4$, the injection ratio for both channels $|E_0^{in}|^2 = |a_i|^2 = -30$ dB, and the steady-state laser output power $P_0 = 1$ mW. A comparison with the analytical small-signal approach, such as in Fig. 5, shows a good agreement. The numerical solution for even smaller channel spacing at the same injection ratio shows that the locking becomes unstable and indicates the limits of the model (Fig. 4).

The crosstalk noise of a typical DFB laser (with the second-order grating, length of 322 μm, effective index of 3.23, K factor

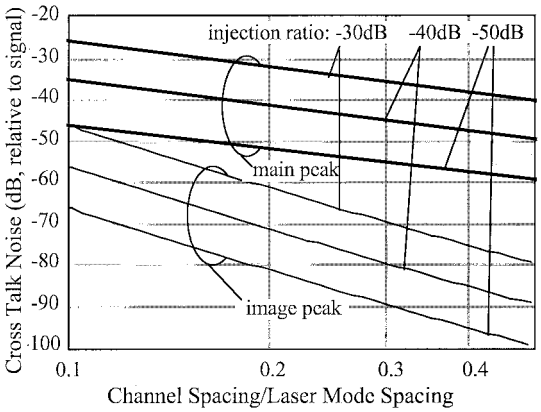

Fig. 6. DFB laser crosstalk noise versus channel spacing.

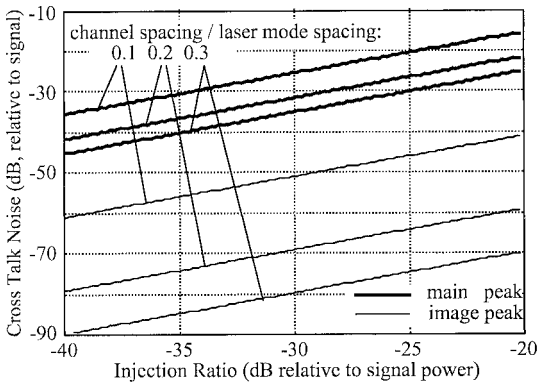

Fig. 7. DFB laser crosstalk noise versus injection ratio.

of 23/cm, 0.2% and 30% reflection on its facets, respectively, and estimated linewidth enhancement factor of 5.4, internal loss of 50/cm) is also modeled. The crosstalk noise against various parameters has been plotted in Figs. 6–8.

From (17), we find that the crosstalk noise is mainly contributed by three mechanisms. The first, the perturbation injection field, feeds through the slave laser cavity, which acts as a filter and is characterized by a transform function $(\mathrm{j}\omega+\mathrm{E}_0^{\mathrm{in}})^{-1}$. This mechanism is dominant for large channel spacing and only contributes to the main noise peak, which coincides with the perturbation injection field. The second mechanism, the perturbance on the magnitude of the injection field, i.e., the injection photon number, modulates the carrier number by changing carrier recombination time. Finally, the perturbance on the magnitude of the injection field also modulates the gain due to gain suppression effect. Those two mechanisms, quantified by $\mathrm{Z_n}(\omega)$ and $\mathrm{Z_p}(\omega)$ and attenuated when fed through the cavity, contribute to both main and image noise peaks and only become dominant for small channel spacing, because of the long carrier lifetime.

Another interesting result is that when the channel spacing is further reduced (of course, the injection ratio must be very low to meet the small perturbance requirements), a response peak has been found around Ω (Fig. 9). This is expected due to the carrier–photon interaction described as the gain saturation relaxation mechanisms [19].

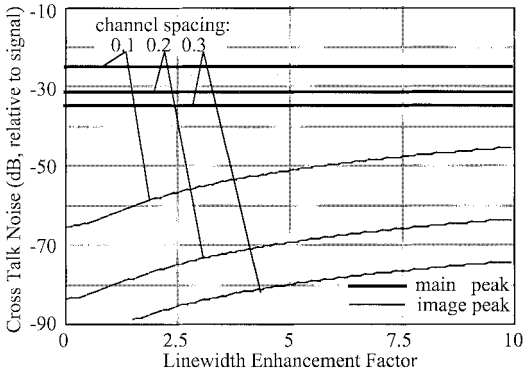

Fig. 8. DFB laser crosstalk noise versus linewidth enhancement factor.

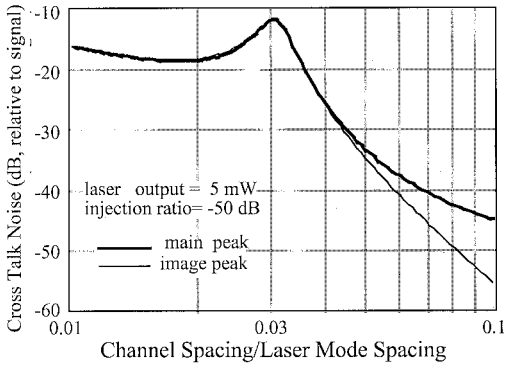

Fig. 9. DFB laser crosstalk noise peak due to gain saturation relaxation.

Finally, we consider a multiple injection line situation. Assume there are a total of N channels with equal spacing ω. $\mathrm{a_i}$ is the complex amplitude of the ith channel and $|\mathrm{a_i}| = \mathrm{a}$. The slave laser is locked to the kth channel. The output of the slave laser will consist of a locked output signal at the kth channel and noise peak at all other channels. From (17), the noise amplitude at the ith channel is

$$\mathrm{e_i} = \frac{\mathrm{a_i} + \mathrm{Z}\left[(\mathrm{i}-\mathrm{k})\omega\right]\frac{(\mathrm{a_i}+\mathrm{a}^*_{2\mathrm{k}-\mathrm{i}})}{2}}{\mathrm{j}(\mathrm{i}-\mathrm{k})\omega + \mathrm{a_k}}.$$

As the noise declines with the very fast increase of frequency, we only consider two strongest noise peaks at the k+1 and k−1 channels

$$\mathrm{e_{k+1}} = \frac{\mathrm{a_{k+1}} + \mathrm{Z}(\omega)\frac{(\mathrm{a_{k+1}}+\mathrm{a}^*_{\mathrm{k-1}})}{2}}{\mathrm{j}\omega + \mathrm{a_k}}$$

$$\mathrm{e_{k-1}} = \frac{\mathrm{a_{k-1}} + \mathrm{Z}(-\omega)\frac{(\mathrm{a_{k-1}}+\mathrm{a}^*_{\mathrm{k+1}})}{2}}{-\mathrm{j}\omega + \mathrm{a_k}}.$$

If the channel reference is generated by FM sideband with modulation index $\Delta \Rightarrow \infty$, we have

$$\mathrm{a_{k-1}} + \mathrm{a}^*_{\mathrm{k+1}} = \mathrm{a_{k+1}} + \mathrm{a}^*_{\mathrm{k-1}} = \frac{2\mathrm{k}}{\Delta}\mathrm{a_k} \Rightarrow 0.$$

The total noise contribution from both peaks is

$$\mathrm{e_n} = \mathrm{e_{k+1}} + \mathrm{e_{k-1}} = \frac{\mathrm{a}^2}{\omega^2 + \mathrm{a}^2}.$$

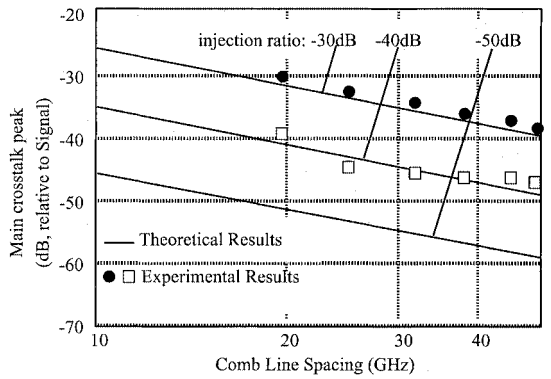

Fig. 10. Comparison between calculated and measured results of relative signal peak power.

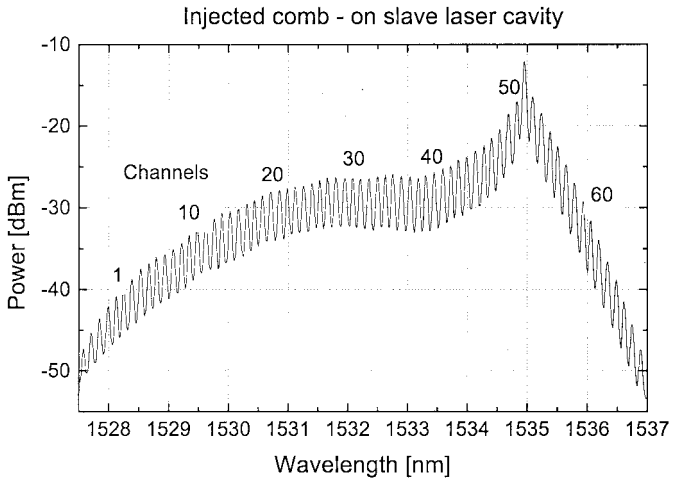

Fig. 11. Optical frequency comb measured before SG-DBR laser.

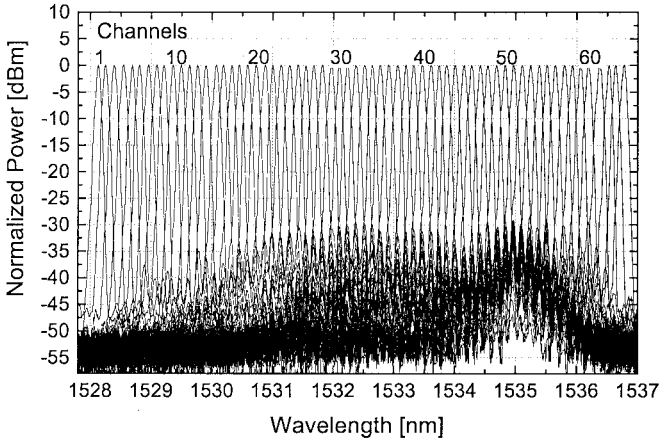

Fig. 12. Superposed SG-DBR for 64 channel filtered output signal.

This is because for the FM signal, the total photon number is always constant; therefore, the carrier and gain modulation contributed by photon number perturbance do not occur. This also implies that the crosstalk range for each channel is limited to its immediate neighbors. Experiments were carried out to verify the modeling results. The results, plotted in Fig. 10, show a good agreement between the model and experiments.

Finally, Figs. 11 and 12 show the results of a practical implementation of the proposed system shown in Fig. 1. Fig. 11 shows

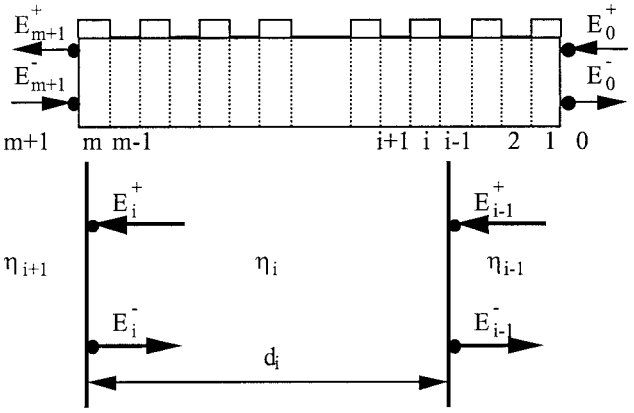

Fig. 13. Transmission-line model of laser structure.

the optical spectrum of the injected signal: the output of an optical comb generator with a comb line spacing up to 25 GHz, here 18 GHz, covering more than 1 THz total frequency range [20]. Fig. 12 shows 64 adjacent superimposed channels formed by injection locking of a widely tunable sampled-grating DBR laser to the optical comb generator spectra. Adjacent channel crosstalk is seen to be suppressed by at least 30 dB for all 64 channels [3].

V. Conclusion

In this paper, we have described a novel approach for WDM channel generation. A small-signal model to deal with wide spectral band optical injection problems has been developed. Based on this model, the crosstalk noise of an injection locked laser in a coherent WDM system is assessed analytically. The results show that the noise is contributed by adjacent injection line "passthrough" effect, carrier number modulation effect, and gain suppression effect. The results also indicate that for injection lines generated by FM side bands, the crosstalk noise is only caused by injection line feed through the slave laser cavity and the crosstalk range is limited to immediate adjacent channels. The static locking range and dynamic stability related to this approach have also been discussed. Experimental results on locking range, stability, and crosstalk noise have confirmed our modeling results, which indicate that stable and low-noise channels can be generated by this approach.

Appendix

Transmission Line Description of DFB Lasers

In DFB or, in fact, any laser structures, the laser resonator can be divided into many small sections, as illustrated by Fig. 13. Each section has uniform refractive index, gain, loss, photon density, carrier density, and carrier injection rate. The electromagnetic field in each section, then, can be determined by transferring the border conditions (i.e., optical emission and injection at laser output facets) to relevant sections. The transfer matrix for section i reads

$$\mathrm{T_i} = \begin{bmatrix} \cos\delta_\mathrm{i} & \mathrm{j}\sin\frac{\delta_\mathrm{i}}{\eta_\mathrm{i}} \\ \mathrm{j}\sin\delta_\mathrm{i}\eta_\mathrm{i} & \cos\delta_\mathrm{i} \end{bmatrix}$$

where $\eta_i = n_{gi} - jk_i$, $k_i = (\alpha_{ai} - g_i)c/2\omega_0$, $\delta_i = \omega_0 \eta_i d_i / c$, and n_{gi}, α_{ai}, g_i, and d_i are the refractive index, absorption, gain coefficient, and length of section i. The relationship of the electric field between section i and i$-$1 is

$$\begin{bmatrix} E_{i-1}^{+} + E_{i-1}^{-} \\ \left(E_{i-1}^{+} + E_{i-1}^{-}\right)\eta_{i-1} \end{bmatrix} = T_i \begin{bmatrix} E_i^{+} + E_i^{-} \\ \left(E_i^{+} + E_i^{-}\right)\eta_i \end{bmatrix}.$$

For a laser with m sections, the steady solution can be obtained by solving

$$\begin{bmatrix} E_0^{+} + E_0^{-} \\ \left(E_0^{+} - E_0^{-}\right)\eta_0 \end{bmatrix} = T_1 T_2 \cdots T_{m-1} T_m \begin{bmatrix} E_{m+1}^{+} - E_{m+1}^{-} \\ \left(E_{m+1}^{+} - E_{m+1}^{-}\right)\eta_{m+1} \end{bmatrix}.$$

At the output side $E_{m+1}^{-} = 0$, the above equation becomes

$$\begin{bmatrix} E_0^{+} + E_0^{-} \\ \left(E_0^{+} - E_0^{-}\right)\eta_0 \end{bmatrix} = T_1 T_2 \cdots T_{m-1} T_m \begin{bmatrix} 1 \\ \eta_{m+1} \end{bmatrix} E_{m+1}^{+}$$

and

$$r = \frac{E_0^{+}}{E_0^{-}}.$$

REFERENCES

[1] M. Chbat and D. Penninck, "High-spectral-efficiency transmission systems," in *Optical Fiber Conf. (OFC2000)*, 2000, pp. 134–136.

[2] B. Cai and A. J. Seeds, "Cross talk noise analysis in optically injection locked semiconductor lasers," in *SIOE '94*, Cardiff, 1994.

[3] S. Fukushima, C. F. C. Silva, Y. Muramoto, and A. J. Seeds, "Optoelectronic synthesis of milliwatt-level multi-octave millimeter-wave signals using an optical frequency comb generator and a unitraveling-carrier photodiode," *IEEE Photon. Technol. Lett.*, vol. 13, pp. 720–722, Jul. 2001.

[4] K. Kikuchi, C. E. Zah, and T. P. Lee, "Amplitude-modulation sideband injection locking characteristics of semiconductor lasers and their application," *J. Lightwave Technol.*, vol. 6, pp. 1821–1830, 1988.

[5] S. Kobayashi and T. Kimura, "Coherence of injection phase-locked AlGaAs semiconductor laser," *Electron. Lett.*, vol. 16, pp. 668–670, 1980.

[6] ——, "Injection locking characteristics of an AlGaAs semiconductor laser," *IEEE J. Quantum Electron.*, vol. QE-16, pp. 915–917, 1980.

[7] K. Iwashita and K. Nakagawa, "Suppression of mode partition noise by laser diode light injection," *IEEE J. Quantum Electron.*, vol. QE-18, pp. 1669–1674, 1982.

[8] F. Mogensenhn, H. Olesen, and G. Jacobseb, "FM. Noise suppression and linewidth reduction in an injection locked semiconductor laser," *Electron. Lett.*, vol. 21, pp. 696–697, 1985.

[9] Y. Yamamoto and T. Kimura, "Coherent optical fiber transmission systems," *IEEE J. Quantum Electron.*, vol. QE-17, pp. 919–935, 1981.

[10] L. Goldberg, H. L. Taylor, J. F. Weller, and D. R. Scifres, "Injection locking of coupled-stripe diode laser arrays," *Appl. Phys. Lett.*, vol. 46, pp. 236–238, 1985.

[11] P. Spano, S. Piazzolla, and M. Tamburrini, "Frequency and intensity noise in injection-locked semiconductor lasers: theory and experiments," *IEEE J. Quantum Electron.*, vol. QE-22, pp. 427–435, 1986.

[12] S. Piazzolla, P. Spano, and M. Tamburrini, "Small signal analysis of frequency chirping in injection-locked semiconductor lasers," *IEEE J. Quantum Electron.*, vol. QE-22, pp. 2219–2223, 1986.

[13] N. Schunk and K. Petermann, "Noise analysis of injection-locked semiconductor injection lasers," *IEEE J. Quantum Electron.*, vol. QE-22, pp. 642–650, 1986.

[14] O. Lidoyne, P. Gallion, C. Chabran, and G. Debarge, "Locking range, phase noise and power spectrum of an injection-locked semiconductor laser," *Proc. Inst. Elect. Eng. J.*, vol. 137, pp. 147–154, 1990.

[15] J. Troger, L. Thevenaz, P. Nicati, and P. Robert, "Theory and experiment of a single-mode diode laser subject to external light injection from several lasers," *J. Lightwave Technol.*, vol. 17, pp. 629–636, 1999.

[16] R. Lang, "Injection locking properties of a semiconductor laser," *IEEE J. Quantum Electron.*, vol. QE-18, pp. 976–983, 1982.

[17] B. Tromborg, H. Olesen, X. Pan, and S. Saito, "Transmission line description of optical feedback and injection locking for Fabry-Pérot and DFB lasers," *IEEE J. Quantum Electron.*, vol. QE-23, pp. 1875–1889, 1987.

[18] I. Gladwell and D. K Sayers, *Computational Technoques for Ordinary Differential Equations*. London, U.K.: Academic, 1980.

[19] K. Vahala and A. Yariv, "Semiclassical theory of noise in semiconductor lasers—Part II," *IEEE J. Quantum Electron.*, vol. QE-19, pp. 1102–1109, 1983.

[20] S. Bennett, B. Cai, E. Burr, O. Gough, and A. J. Seeds, "1.8-THz bandwidth, zero-frequency error, tunable optical comb generator for DWDM applications," *IEEE Photon. Technol. Lett.*, vol. 11, pp. 551–553, May 1999.

B. Cai, photograph and biography not available at the time of publication.

L. A. Johansson received the M.Sc. degree from the Royal Institute of Technology (KTH), Stockholm, Sweden, in 1997 and the Ph.D. degree from University College London (UCL), London, U.K., in 2002.

In 2002, he joined the University of California, Santa Barbara, in a postdoctoral position. His reseach interests at UCL include design and characterization of integrated photonic devices for analog and digital applications.

C. F. C. Silva, photograph and biography not available at the time of publication.

S. Bennett, photograph and biography not available at the time of publication.

Alwyn J. Seeds (M'81–SM'92–F'97) received the Ph.D. and D.Sc.(Eng.) degrees from the University of London, London, U.K., in 1980 and 2002, respectively.

From 1980 to 1983, he was a Staff Member at Lincoln Laboratory, Massachusetts Institute of Technology (MIT), Cambridge, where he worked on GaAs monolithic millimeter-wave integrated circuits for use in phased-array radar. He returned to the U.K. in 1983 to lecture in telecommunications at Queen Mary College, University of London. He then moved to University College London in 1986, where he is currently Professor of optoelectronics and Head of the Opto-electronics and Optical Networks Group. He has published more than 200 papers on microwave and optoelectronic devices and their systems applications and is presenter of the video "Microwave Opto-electronics" in the *IEEE Emerging Technologies* series. His current research interests include microwave bandwidth tuneable semiconductor lasers, semiconductor optical modulators, optical control of microwave devices, mode-locked lasers, optical phase-lock loops, optical frequency synthesis, broad-band radio over fiber access systems, dense wavelength-division-multiplexing (WDM) networks, and all-optical signal regeneration.

Prof. Seeds is Chairman of the Institution of Electrical Engineers (IEE) Photonics Professional Network and has served on the program committees for many international conferences.